Electromagnetic energy within coated spheres containing dispersive metamaterials

Tiago José Arruda,[1] Felipe A. Pinheiro,[2] and Alexandre Souto Martinez[1,3,*]

[1]*Faculdade de Filosofia, Ciências e Letras de Ribeirão Preto,*

Universidade de São Paulo

Avenida Bandeirantes, 3900

14040-901, Ribeirão Preto, São Paulo, Brazil

[2]*Instituto de Física, Universidade Federal do Rio de Janeiro,*

Rio de Janeiro-RJ, 21941-972, Brazil

[3]*National Institute of Science and Technology in Complex Systems*

Abstract

An exact expression for the time-averaged electromagnetic energy within a magneto-dielectric coated sphere, which is irradiated by a plane and time-harmonic electromagnetic wave, is derived. Both the spherical shell and core are considered to be dispersive and lossy, with a realistic dispersion relation of an isotropic non-Lorentz-type split-ring resonator metamaterial. As an application, we calculate the energy-transport velocity in a disordered medium consisting of dispersive and lossy metamaterial coated spheres.

OCIS codes: 290.0290, 290.4020, 290.5825, 290.5850, 160.3918.

*Corresponding author: asmartinez@ffclrp.usp.br

1. Introduction

Electromagnetic (EM) scattering by small particles is a fundamental topic in classical electrodynamics. It has a broad range of applications, including biology, meteorology, astronomy, and medicine. Historically, a complete solution for homogeneous spheres with arbitrary size was first derived, in an independent way, by Lorenz and Mie more than a century ago [1, 2]. For this reason, this solution is today widely known as Lorenz-Mie solution. Despite its long history, the research on EM scattering still reveals surprises. Giant resonances that anomalously increase with the resonances order (dipole, quadrupole, etc.) [3], the formation of complex field structures with vortices inside scattering particles [4], and the superscattering of light in subwavelength structures, in which the single-channel limit can be overcome [5], are some examples of interesting, unexpected, and basic phenomena that have been recently unveiled in the field of EM scattering.

Most of these recent results have been driven by the extraordinary technological progresses in the emerging field of nanophotonics. In this field, the understanding of the interaction between EM radiation and individual nanostructures is crucial. Indeed, one of the most important challenges is to confine light at the subwavelength scale, leading to an enhancement of the EM field. The excitation of plasmons localized at the surface of nanoparticles is a common strategy to achieve such enhancement [6]. The investigation of EM scattering by metallic nanoparticles provides important insights on the understanding and control of the excitation of surface plasmons. It allows the optimization of the field enhancement, and hence the design of novel photonic devices. One important example is the metallic coated spherical nanoparticle. The Lorenz-Mie solution for this geometry, first obtained by Aden

and Kerker [7], provides the theoretical basis for many applications, such as the radiative heat transfer at the nanoscale [8], the off-resonance field enhancement in EM scattering [9], and the spaser-based nanolaser [10].

In the last decade, the development of metamaterials has opened up new frontiers in photonics. Metamaterials exhibit unusual optical properties, with no counterpart in natural media, that can be exploited to generate negative refraction [11], resolve images beyond the diffraction limit [12], exhibit optical magnetism [13, 14], and act as an electromagnetic cloak [15, 16]. As many fundamental aspects of classical electrodynamics, EM scattering has been revised due the advent of metamaterials and the possibility of negative refraction [17–19]. Interestingly, it was demonstrated that negative refraction is at the origin of departures from the well-known Rayleigh law [19]. The related problem of the EM energy density stored in dispersive metamaterials, including unavoidable losses and realistic effective constitutive parameters for both split-ring-resonators (SRR) [20–22] and chiral metamaterials [23], has been treated recently. As far as we are aware, the case of the EM energy density within coated spheres, an important geometry for applications in photonics, made of metamaterials has never been treated so far.

The aim of the this paper is to fill this gap by investigating the EM energy density within coated spheres made of dispersive metamaterials, including losses and realistic material parameters. To accomplish this, we use the magnetic Aden-Kerker solution [1] for the internal EM field to obtain an exact expression for the time-averaged EM energy within a dispersive spherical shell and core. This generalizes the results already obtained for homogeneous spheres irradiated by plane waves [24–27], and allow us to analyze the resonances inside

the core and shell separately. Both dispersion and losses are taken into account, as well as realistic effective parameters for wires-SRR metamaterials.

This paper is organized as follows. In Sec. 2, the expressions of the internal EM field inside the coated sphere are explicitly derived. Section 3 is devoted to the calculation of the time-averaged EM energy density, the main result of this paper. The dispersion relations associated with a wires-SRR metamaterial are presented in Sec. 4. Section 5 is reserved to the numerical results whereas in Sec. 6 we provide a summary of our main conclusions.

2. Aden-Kerker solution

Let $(\mathbf{E}, \mathbf{H})$ be a plane and complex EM wave with time-harmonic dependence $\exp(-\imath\omega t)$, where ω is the angular frequency, and electric field amplitude is E_0. This wave is incident to a magneto-dielectric coated sphere with inner radius a and outer one b. The involved media are assumed to be linear, homogeneous and isotropic, with scalar electric permittivity and magnetic permeability (ϵ_1, μ_1) for the core $(0 \leq r \leq a)$, (ϵ_2, μ_2) for the spherical shell $(a \leq r \leq b)$, and (ϵ_0, μ_0) for the surrounding medium $(r \geq b)$, with the last one considered to be the free-space [1]. Under these assumptions, the macroscopic Maxwell's equations for non-optically active media provide the vector Helmholtz equation $[\nabla^2 + k^2](\mathbf{E}, \mathbf{H}) = (\mathbf{0}, \mathbf{0})$, where $k = 2\pi/\lambda$ is the wave number and λ is the wavelength of the radiation in the respective medium. The solutions of this equation for each region above delimited, which are a generalization of the Lorenz-Mie solutions [1, 2], are known as the Aden-Kerker solutions [1, 7]. Solving this vector equation, the scalar components of the internal EM fields $(\mathbf{E}_q, \mathbf{H}_q)$ in the spherical coordinate system (r, θ, ϕ) inside the spherical core $(q = 1)$ and shell $(q = 2)$ are explicitly given [1, 7, 26]:

$$E_{qr} = -\frac{\imath \cos\phi \sin\theta}{\rho_q^2} \sum_{n=1}^{\infty} E_n n(n+1)\pi_n \left\{\delta_{1,q} d_n \psi_n(\rho_q) + \delta_{2,q} \left[g_n \psi_n(\rho_q) - w_n \chi_n(\rho_q)\right]\right\} \ , \quad (1)$$

$$E_{q\theta} = \frac{\cos\phi}{\rho_q} \sum_{n=1}^{\infty} E_n \big(\delta_{1,q} \left[c_n \pi_n \psi_n(\rho_q) - \imath d_n \tau_n \psi_n'(\rho_q)\right] + \delta_{2,q} \left\{\pi_n \left[f_n \psi_n(\rho_q) - v_n \chi_n(\rho_q)\right] - \imath \tau_n \left[g_n \psi_n'(\rho_q) - w_n \chi_n'(\rho_q)\right]\right\}\big) \ , \quad (2)$$

$$E_{q\phi} = \frac{\sin\phi}{\rho_q} \sum_{n=1}^{\infty} E_n \big(\delta_{1,q} \left[\imath d_n \pi_n \psi_n'(\rho_q) - c_n \tau_n \psi_n(\rho_q)\right] + \delta_{2,q} \left\{\imath \pi_n \left[g_n \psi_n'(\rho_q) - w_n \chi_n'(\rho_q)\right] - \tau_n \left[f_n \psi_n(\rho_q) - v_n \chi_n(\rho_q)\right]\right\}\big) \ , \quad (3)$$

$$H_{qr} = -\frac{\imath k_q \sin\phi \sin\theta}{\omega \mu_q \rho_q^2} \sum_{n=1}^{\infty} E_n n(n+1)\pi_n \left\{\delta_{1,q} c_n \psi_n(\rho_q) + \delta_{2,q} \left[f_n \psi_n(\rho_q) - v_n \chi_n(\rho_q)\right]\right\} \ , \quad (4)$$

$$H_{q\theta} = \frac{k_q \sin\phi}{\omega \mu_q \rho_q} \sum_{n=1}^{\infty} E_n \big(\delta_{1,q} \left[d_n \pi_n \psi_n(\rho_q) - \imath c_n \tau_n \psi_n'(\rho_q)\right] + \delta_{2,q} \left\{\pi_n \left[g_n \psi_n(\rho_q) - w_n \chi_n(\rho_q)\right] - \imath \tau_n \left[f_n \psi_n'(\rho_q) - v_n \chi_n'(\rho_q)\right]\right\}\big) \ , \quad (5)$$

$$H_{q\phi} = \frac{k_q \cos\phi}{\omega \mu_q \rho_q} \sum_{n=1}^{\infty} E_n \big(\delta_{1,q} \left[d_n \tau_n \psi_n(\rho_q) - \imath c_n \pi_n \psi_n'(\rho_q)\right] + \delta_{2,q} \left\{\tau_n \left[g_n \psi_n(\rho_q) - w_n \chi_n(\rho_q)\right] - \imath \pi_n \left[f_n \psi_n'(\rho_q) - v_n \chi_n'(\rho_q)\right]\right\}\big) \ , \quad (6)$$

where $\rho_q = k_q r$, with k_q being the wave number in the medium (ϵ_q, μ_q), $\delta_{q,q'}$ is the Kronecker delta and $E_n = \imath^n E_0(2n+1)/[n(n+1)]$ [1]. The radial functions $\psi_n(\rho_q) = \rho_q j_n(\rho_q)$ and $\chi_n(\rho_q) = -\rho_q y_n(\rho_q)$ are the Riccati-Bessel and Riccati-Neumann functions, respectively, where j_n is the spherical Bessel function and y_n is the Neumann function. The angular functions are $\pi_n = P_n^1(\cos\theta)/\sin\theta$ and $\tau_n = \mathrm{d}[P_n^1(\cos\theta)]/\mathrm{d}\theta$, where P_n^1 is the associated Legendre function of first order. The expressions for the incident and scattered EM fields in terms of vector spherical harmonics and the scattering coefficients a_n and b_n can be found in [1].

Imposing the continuity of the tangential components of the EM fields at the interfaces ($r = a$ and $r = b$) between the media, we obtain the multipole moments, known as the Aden-Kerker coefficients, in the magnetic approach ($\mu_q \neq \mu_0$) [1, 7]:

$$a_n = \frac{\widetilde{m}_2\psi_n'(y)\alpha_n - \psi_n(y)\widetilde{\alpha}_n}{\widetilde{m}_2\xi_n'(y)\alpha_n - \xi_n(y)\widetilde{\alpha}_n} , \tag{7}$$

$$b_n = \frac{\psi_n'(y)\beta_n - \widetilde{m}_2\psi_n(y)\widetilde{\beta}_n}{\xi_n'(y)\beta_n - \widetilde{m}_2\xi_n(y)\widetilde{\beta}_n} , \tag{8}$$

$$c_n = \frac{m_1 f_n \beta_n}{m_2\psi_n(m_1 x)} , \tag{9}$$

$$d_n = \frac{m_1 g_n \widetilde{\alpha}_n}{m_2\psi_n'(m_1 x)} , \tag{10}$$

$$f_n = \frac{m_2\imath}{\xi_n'(y)\beta_n - \widetilde{m}_2\xi_n(y)\widetilde{\beta}_n} , \tag{11}$$

$$g_n = \frac{m_2\imath}{\widetilde{m}_2\xi_n'(y)\alpha_n - \xi_n(y)\widetilde{\alpha}_n} , \tag{12}$$

$$v_n = B_n f_n , \tag{13}$$

$$w_n = A_n g_n , \tag{14}$$

with the auxiliary functions expressed by

$$A_n = \frac{\widetilde{m}_2\psi_n(m_2x)\psi_n'(m_1x) - \widetilde{m}_1\psi_n'(m_2x)\psi_n(m_1x)}{\widetilde{m}_2\chi_n(m_2x)\psi_n'(m_1x) - \widetilde{m}_1\chi_n'(m_2x)\psi_n(m_1x)} ,$$

$$B_n = \frac{\widetilde{m}_2\psi_n'(m_2x)\psi_n(m_1x) - \widetilde{m}_1\psi_n(m_2x)\psi_n'(m_1x)}{\widetilde{m}_2\chi_n'(m_2x)\psi_n(m_1x) - \widetilde{m}_1\chi_n(m_2x)\psi_n'(m_1x)} ,$$

$$\alpha_n = \psi_n(m_2y) - A_n\chi_n(m_2y) ,$$

$$\beta_n = \psi_n(m_2y) - B_n\chi_n(m_2y) ,$$

$$\widetilde{\alpha}_n = \psi_n'(m_2y) - A_n\chi_n'(m_2y) ,$$

$$\widetilde{\beta}_n = \psi_n'(m_2y) - B_n\chi_n'(m_2y) .$$

The quantities $x = ka$ and $y = kb$ are the size parameters related to the inner and the outer spheres, respectively, with k being the incident wave number. The function $\xi_n(\rho_q) = \psi_n(\rho_q) -$

$\imath\chi_n(\rho_q)$ is the Riccati-Hankel function. The refractive and impedance indices are $m_q = k_q/k = [\epsilon_q\mu_q/(\epsilon_0\mu_0)]^{1/2}$ and $\widetilde{m}_q = \mu_0 m_q/\mu_q = [\epsilon_q\mu_0/(\epsilon_0\mu_q)]^{1/2}$ [28–30], respectively (with $q = 1$ for the core and $q = 2$ for the shell). In particular, for numerical calculations involving materials with negative refractive indices (the real parts of permittivity and permeability are both negative), it is convenient to write $m_q = (\epsilon_q/\epsilon_0)^{1/2}(\mu_q/\mu_0)^{1/2}$, since $\imath^2 = -1$ and, thereby, $\mathrm{Re}(m_q) < 0$. Note that, for a homogeneous sphere, *i.e.*, $m_1 = m_2$ and $\widetilde{m}_1 = \widetilde{m}_2$, one has $A_n = B_n = 0$ and, therefore, the usual Lorenz-Mie coefficients are recovered [1]. The same result holds either in the limit of zero core ($a \to 0$, homogeneous sphere of radius b) or zero shell ($a \to b$, homogeneous sphere of radius $a = b$) [1].

3. Time-averaged internal energy

Consider a time-harmonic EM field $(\mathbf{E}_q, \mathbf{H}_q)$ confined to a homogeneous and isotropic medium which is restricted to a spherical shell ($l_1 \leq r \leq l_2$), with complex optical constants $\epsilon_q = \epsilon_q' + \imath\epsilon_q''$ and $\mu_q = \mu_q' + \imath\mu_q''$. The time-averaged EM energy ($W_q = \langle W_q\rangle_t$) stored inside this region can be calculated by means of the equation [31]

$$W_q(l_1, l_2) = \int_0^{2\pi} \mathrm{d}\phi \int_{-1}^{1} \mathrm{d}(\cos\theta) \int_{l_1}^{l_2} \mathrm{d}r\; r^2 \langle u_q\rangle_t \;, \tag{15}$$

where $\langle u_q\rangle_t = \langle u_q\rangle_t(r, \cos\theta, \phi)$ is the corresponding time-averaged energy density:

$$\langle u_q\rangle_t = \frac{1}{4}\left[\epsilon_q^{(\mathrm{eff})}\,|\mathbf{E}_q|^2 + \mu_q^{(\mathrm{eff})}\,|\mathbf{H}_q|^2\right] \;, \tag{16}$$

with $\epsilon_q^{(\mathrm{eff})}$ and $\mu_q^{(\mathrm{eff})}$ being the effective electric and magnetic energy coefficients, respectively [21]. Specially, for dispersive and weakly absorbing medium ($\epsilon_q' \gg \epsilon_q''$, $\mu_q' \gg \mu_q''$), one

has the positive definite coefficients [31]

$$\epsilon_q^{(\mathrm{eff})}(\omega) \;=\; \frac{\partial\left[\omega\epsilon_q'(\omega)\right]}{\partial\omega} > 0\;, \tag{17}$$

$$\mu_q^{(\mathrm{eff})}(\omega) \;=\; \frac{\partial\left[\omega\mu_q'(\omega)\right]}{\partial\omega} > 0\;. \tag{18}$$

If the lossless medium (ϵ_q, μ_q) is also non-dispersive, one readily obtains $\epsilon_q^{(\mathrm{eff})} = \epsilon_q'$ and $\mu_q^{(\mathrm{eff})} = \mu_q'$ from Eqs. (17) and (18) [24, 31]. To guarantee the positiveness of the EM energy density, this last result imposes that materials with both $\epsilon_q' < 0$ and $\mu_q' < 0$ are necessarily dispersive. We stress that, for lossy and dispersive materials, however, the quantities $[\epsilon_q^{(\mathrm{eff})}, \mu_q^{(\mathrm{eff})}]$ in Eq. (16) cannot be calculated using Eqs. (17) and (18). Indeed, these quantities depend on the approach and the model used to describe the dispersion relations [21, 31].

If the shell has the same optical properties as the surrounding medium (ϵ_0, μ_0), which is assumed to be non-dispersive and non-absorbing, one has

$$W_0(l_1, l_2) = \frac{2}{3}\pi|E_0|^2\epsilon_0(l_2^3 - l_1^3)\;. \tag{19}$$

In addition, for $m_q \neq m_q^*$ $(q = \{1, 2\})$, one has an analytical expression for the integral that appears in the radial part of Eq. (15), which involves product of the spherical Bessel and Neumann functions [32]. For sake of simplicity, we define the dimensionless function [26, 27, 33]

$$\begin{aligned}\frac{\mathcal{I}_{q,n}^{(z\bar{z})}(l_1, l_2)}{1/(l_2^3 - l_1^3)} &= \int_{l_1}^{l_2} \mathrm{d}r\; r^2 z_n(\rho_q)\bar{z}_n(\rho_q^*) \\ &= r^3\,\frac{\left[\rho_q^* z_n(\rho_q)\bar{z}_n'(\rho_q^*) - \rho_q z_n'(\rho_q)\bar{z}_n(\rho_q^*)\right]}{\rho_q^2 - \rho_q^{*2}}\Bigg|_{r=l_1}^{r=l_2},\end{aligned} \tag{20}$$

where z_n e $\bar{z}_n$ may be any spherical Bessel or Neumann functions, and $l_1, l_2 \in \mathbb{R}$ are the limits of integration. In the situation, in which $m_q = \pm m_q^*$ $(q = \{1, 2\})$, using L'Hospital's

rule and recurrence relations involving spherical Bessel and Neumann functions [32], we obtain

$$\begin{aligned}\frac{\mathcal{I}_{q,n}^{(z\bar{z})}(l_1,l_2)}{1/(l_2^3-l_1^3)} &= \lim_{m_q\to\pm m_q^*}\int_{l_1}^{l_2}\mathrm{d}r\; r^2 z_n(m_q kr)\bar{z}_n(m_q^* kr)\\ &= \varrho_{\pm,n}^{(z\bar{z})}\frac{r^3}{4}\big[2z_n(\rho_q)\bar{z}_n(\rho_q)-z_{n-1}(\rho_q)\bar{z}_{n+1}(\rho_q)\\ &\quad -z_{n+1}(\rho_q)\bar{z}_{n-1}(\rho_q)\big]\Big|_{r=l_1}^{r=l_2},\end{aligned} \tag{21}$$

where one must necessarily choose $\varrho_{+,n}^{(z\bar{z})}=1$, for $m_q=m_q^*$ [*i.e.*, $\mathrm{Im}(m_q)=0$]. For $m_q=-m_q^*$ [$\mathrm{Re}(m_q)=0$], according to the definition in Eq. (21), one has the following combinations: $\varrho_{-,n}^{(jj)}=\varrho_{-,n}^{(yj)}=(-1)^n$ and $\varrho_{-,n}^{(yy)}=\varrho_{-,n}^{(jy)}=(-1)^{n+1}$, since $j_n(-\rho)=(-1)^n j_n(\rho)$ and $y_n(-\rho)=(-1)^{n+1}y_n(\rho)$ [32]. Eqs. (20) and (21) are quite suitable to simplify the expressions associated with the average internal energy [24, 26, 27, 33] and intensities [34], and it is the first time that these general formulations, including both Bessel and Neumann functions, are used in this context of magnetic scatterers.

In the spherical core ($0\leq r\leq a$), separating the electric and magnetic fields contributions to the average EM energy, that is, $W_{1E}\equiv\int_{\mathcal{V}_1}\mathrm{d}^3r\epsilon_1^{(\mathrm{eff})}|\mathbf{E}_1|^2/4$ and $W_{1H}\equiv\int_{\mathcal{V}_1}\mathrm{d}^3r\mu_1^{(\mathrm{eff})}|\mathbf{H}_1|^2/4$, with $\mathcal{V}_1$ being the respective region of integration, we obtain, respectively:

$$\frac{W_{1E}(0,a)}{W_0(0,a)} = \frac{3}{4}\frac{\epsilon_1^{(\mathrm{eff})}}{\epsilon_0}\sum_{n=1}^{\infty}\left\{(2n+1)|c_n|^2\mathcal{I}_{1,n}^{(jj)}(0,a)+|d_n|^2\left[n\mathcal{I}_{1,n+1}^{(jj)}(0,a)+(n+1)\mathcal{I}_{1,n-1}^{(jj)}(0,a)\right]\right\}, \tag{22}$$

$$\frac{W_{1H}(0,a)}{W_0(0,a)} = \frac{3}{4}|\widetilde{m}_1|^2\frac{\mu_1^{(\mathrm{eff})}}{\mu_0}\sum_{n=1}^{\infty}\left\{(2n+1)|d_n|^2\mathcal{I}_{1,n}^{(jj)}(0,a)+|c_n|^2\left[n\mathcal{I}_{1,n+1}^{(jj)}(0,a)+(n+1)\mathcal{I}_{1,n-1}^{(jj)}(0,a)\right]\right\}, \tag{23}$$

where we have used Eqs. (1)–(6), (15), (19) and (20) [or (21)] for $q=1$, $l_1=0$ and $l_2=a$. The radial and angular contributions have been simplified by applying the relations $(2n+1)\int_{-1}^{1}\mathrm{d}(\cos\theta)\pi_n\pi_{n'}\sin^2\theta=2n(n+1)\delta_{n,n'}$, $(2n+1)\int_{-1}^{1}\mathrm{d}(\cos\theta)(\pi_n\pi_{n'}+\tau_n\tau_{n'})=$

$2n^2(n+1)^2\delta_{n,n'}$ and $\int_{-1}^{1} \mathrm{d}(\cos\theta)(\pi_n\tau_{n'} + \tau_n\pi_{n'}) = 0$ [1, 26]. Therefore, from Eqs. (22) and (23), we calculate the average EM energy within the core as the sum of the electric and magnetic contributions:

$$W_1(0,a) = W_{1E}(0,a) + W_{1H}(0,a)\ . \tag{24}$$

These results, which are not straightforwardly obtained, are in agreement with the papers of Bott and Zdunkowski [24] in the nonmagnetic approach ($\mu_1 = \mu_0$) and Ruppin [27] for a Lorentz-type permeability. Some details of these calculations for the magnetic case ($\mu_1 \neq \mu_0$) can be found in the paper of Arruda and Martinez [26].

Analogously, in the shell region ($a \leq r \leq b$) we obtain the electric and magnetic contributions to the average EM energy, respectively:

$$\begin{aligned}\frac{W_{2E}(a,b)}{W_0(a,b)} = \frac{3}{4}\frac{\epsilon_2^{(\mathrm{eff})}}{\epsilon_0}\sum_{n=1}^{\infty}\Bigg\{&(2n+1)|f_n|^2\mathcal{I}_{2,n}^{(jj)}(a,b) + |g_n|^2\left[n\mathcal{I}_{2,n+1}^{(jj)}(a,b) + (n+1)\mathcal{I}_{2,n-1}^{(jj)}(a,b)\right]\\ &+(2n+1)|v_n|^2\mathcal{I}_{2,n}^{(yy)}(a,b) + |w_n|^2\left[n\mathcal{I}_{2,n+1}^{(yy)}(a,b) + (n+1)\mathcal{I}_{2,n-1}^{(yy)}(a,b)\right]\\ &+2\mathrm{Re}\Big[(2n+1)f_nv_n^*\mathcal{I}_{2,n}^{(jy)}(a,b) + g_nw_n^*\left(n\mathcal{I}_{2,n+1}^{(jy)}(a,b) + (n+1)\mathcal{I}_{2,n-1}^{(jy)}(a,b)\right)\Big]\Bigg\}\ ,\end{aligned} \tag{25}$$

for the electric field $\mathbf{E}_2$, and

$$\begin{aligned}\frac{W_{2H}(a,b)}{W_0(a,b)} = \frac{3}{4}|\widetilde{m}_2|^2\frac{\mu_2^{(\mathrm{eff})}}{\mu_0}\sum_{n=1}^{\infty}\Bigg\{&(2n+1)|g_n|^2\mathcal{I}_{2,n}^{(jj)}(a,b) + |f_n|^2\left[n\mathcal{I}_{2,n+1}^{(jj)}(a,b) + (n+1)\mathcal{I}_{2,n-1}^{(jj)}(a,b)\right]\\ &+(2n+1)|w_n|^2\mathcal{I}_{2,n}^{(yy)}(a,b) + |v_n|^2\left[n\mathcal{I}_{2,n+1}^{(yy)}(a,b) + (n+1)\mathcal{I}_{2,n-1}^{(yy)}(a,b)\right]\\ &+2\mathrm{Re}\Big[(2n+1)g_nw_n^*\mathcal{I}_{2,n}^{(jy)}(a,b) + f_nv_n^*\left(n\mathcal{I}_{2,n+1}^{(jy)}(a,b) + (n+1)\mathcal{I}_{2,n-1}^{(jy)}(a,b)\right)\Big]\Bigg\}\ ,\end{aligned} \tag{26}$$

for the magnetic field $\mathbf{H}_2$, where we have employed Eqs. (1)–(6), (15), (19) and (20) [or (21)] for $q = 2$, $l_1 = a$ and $l_2 = b$. The average EM energy within the spherical shell is readily calculated by the expression

$$W_2(a,b) = W_{2E}(a,b) + W_{2H}(a,b) \ . \tag{27}$$

From Eqs. (24) and (27), we finally calculate the *effective* time-averaged EM energy within the magneto-dielectric coated sphere as the sum of the average energies stored in the spherical core and shell:

$$W_{1;2}(a,b) = W_1(0,a) + W_2(a,b) \ . \tag{28}$$

Therefore, given the constitutive parameters associated with the media (ϵ_q, μ_q), $q = \{1,2\}$, one can readily determine the respective average EM energy inside the spherical particle by means of Eqs. (22)–(28).

4. Dispersive metamaterial

A composite isotropic metamaterial (ϵ_q, μ_q), consisting of an array of wires and an array of split-ring resonators (SRR), can be described by the *effective* scalar quantities [11]

$$\epsilon_q(\omega) \ = \ \epsilon_0 \left[1 - \frac{\omega_{\rm p}^2}{\omega(\omega + \imath\gamma)}\right] \ , \tag{29}$$

$$\mu_q(\omega) \ = \ \mu_0 \left[1 - \frac{F\omega^2}{(\omega^2 - \omega_0^2) + \imath\omega\Gamma}\right] \ , \tag{30}$$

where $\omega_{\rm p}$ and ω_0 are the effective plasma and resonance frequencies associated with the wire and the SRR media, respectively. The dimensionless factor F is the fractional area of the unit cell occupied by the interior of the split ring, and γ and Γ are damping coefficients.

The constitutive quantities ϵ_0 and μ_0 are the permittivity and the permeability of the free-space, respectively. For a certain frequency band, at the microwave range, the real part of the dispersive quantities in Eqs. (29) and (30) are both negative ($\epsilon'_q < 0, \mu'_q < 0$). These negative parameters lead to a negative index of refraction and the metamaterial is considered to be "left-handed" because, for plane waves propagating through this medium at this frequency range, the wavevector lies in the direction opposite to the EM energy flux, given by the Poynting vector [35]. In the lossless situation, one has explicitly the refractive index $m_q = (\epsilon_q/\epsilon_0)^{1/2}(\mu_q/\mu_0)^{1/2} = p[\epsilon_q\mu_q/(\epsilon_0\mu_0)]^{1/2}$, where $p = -1$ if both ϵ'_q and μ'_q are negative, and $p = 1$ otherwise. It is important to emphasize that metamaterials exhibiting negative refraction must be dispersive to guarantee the positiveness of the EM energy density [35].

From the non-Lorentz-type model provided by the SRR media [11], Eq. (30), and the plasma-like dispersion associated with the wires, Eq. (29), Tretyakov [20] has determined an exact expression for the EM energy density using an equivalent circuit (EC) approach. Both the EC and the electrodynamic (ED) approaches have been discussed by Boardman and Marinov [21], considering the limits of validity of the energy density in metamaterials of Lorentz- and SRR-type. The effective electric and magnetic energy coefficients, which enter Eq. (15), are, in the ED approach, given by [21]: $\epsilon_q^{(\mathrm{eff})}|_{\mathrm{ED}} = \epsilon_0[1 + \omega_{\mathrm{p}}^2/(\omega^2 + \gamma^2)]$ and $\mu_q^{(\mathrm{eff})}|_{\mathrm{ED}} = \mu_0(1 + F\omega^2[\omega_0^2(3\omega_0^2 - \omega^2) + \omega^2\Gamma^2]/\{\omega_0^2[(\omega_0^2 - \omega^2)^2 + \omega^2\Gamma^2]\})$. As pointed out in [21], these energy coefficients in ED approach are in perfect agreement in dispersive and lossless materials ($\gamma = \Gamma = 0$), described by the Landau's classical formula [31] in Eqs. (17) and (18). In EC approach, the effective energy coefficients calculated by Tretyakov [20] are $\epsilon_q^{(\mathrm{eff})}|_{\mathrm{EC}} = \epsilon_q^{(\mathrm{eff})}|_{\mathrm{ED}}$ and $\mu_q^{(\mathrm{eff})}|_{\mathrm{EC}} = \mu_0\{1+F\omega^2(\omega_0^2 + \omega^2)/[(\omega_0^2 - \omega^2)^2 + \omega^2\Gamma^2]\}$, which are more

adequate to describe the low-frequency range $\omega < \omega_0$ than the magnetic energy coefficient provided by the Lorentz-type model [27, 36]: $\mu_q|_{\text{Lorentz}} = \mu_0\{1 - F\omega_0^2/[(\omega^2 - \omega_0^2) + \imath\omega\Gamma]\}$ and $\mu_q^{(\text{eff})}|_{\text{Lorentz}} = \mu_0\{1 + F\omega_0^2(\omega^2 + \omega_0^2)/[(\omega_0^2 - \omega^2)^2 + \omega^2\Gamma^2]\}$. On the other hand, the Lorentz-type dispersion is a more adequate description than the EC approach in the high-frequency range $\omega > \omega_0$ [21]. Both approaches, however, do not satisfy the classical energy formula for dispersive lossless materials in time-harmonic fields.

Recently, Luan [22] has shown that if the power loss is firstly identified, the EC approach reduces to the ED one, and the correct expressions for the effective electric and magnetic energy coefficients, which are consistent with the Landau's classical formula [31], are

$$\epsilon_q^{(\text{eff})}(\omega) = \epsilon_0 \left[1 + \frac{\omega_\text{p}^2}{\omega^2 + \gamma^2}\right] , \tag{31}$$

$$\mu_q^{(\text{eff})}(\omega) = \mu_0 \left[1 + \frac{F\omega^2\left(3\omega_0^2 - \omega^2\right)}{\left(\omega_0^2 - \omega^2\right)^2 + \omega^2\Gamma^2}\right] . \tag{32}$$

In the following, we adopt the constitutive quantities given in Eqs. (29) and (30) to describe a non-Lorentz-type (SRR) metamaterial, and use in the average EM energy [Eq. (15)] the energy coefficients calculated by Luan [22], Eqs. (31) and (32), since they are valid for both EC and ED approaches and contain Eqs. (17) and (18) as particular cases. We emphasize that these calculations involving this particular set of parameters are an application of the analytic results obtained in Secs. 2 and 3, which are generally valid for other classes of dispersive, non-optically active metamaterials in time-harmonic fields.

5. Numerical results

To calculate the time-averaged EM energy as stated in Eq. (28), it is suitable to deal with dimensionless quantities only. From Eqs. (19), (24), (27) and (28), we obtain a normalization

$W_{\rm nor} = W_{1;2}(a,b)/W_0(0,b)$, which yields

$$W_{\rm nor}(S) = S^3 \frac{W_1(0,a)}{W_0(0,a)} + (1-S^3)\frac{W_2(a,b)}{W_0(a,b)} \ , \tag{33}$$

where $S = a/b$ is the thickness ratio of the coated sphere. Note that S^3 and $(1-S^3)$ are the volume fraction of the spherical core and shell, respectively. Here, all the numerical calculations have been performed by a computer code written for the free software *Scilab* 5.3.3. According to Ruppin [17], we choose $f_{\rm p} = 10$ GHz and $f_0 = 4$ GHz for the plasma and magnetic resonance frequencies, respectively. The damping coefficients are assumed to be $\gamma = 0.03\omega_{\rm p}$ and $\Gamma = 0.03\omega_0$, and the dimensionless parameter $F = 0.56$ has been chosen. With this set of parameters, the real parts of the electric permittivity and magnetic permeability are simultaneously negative for $f_0 = 4$ GHz to 6 GHz, so that a band of negative refraction shows up in this frequency range. The extinction efficiency $Q_{\rm ext}$, which is the extinction cross-section in units of the geometric one, can be calculated as follows [1]:

$$Q_{\rm ext} = \frac{2}{y^2}\sum_{n=1}^{\infty}(2n+1){\rm Re}\left(a_n + b_n\right) \ , \tag{34}$$

where $y = kb$ is the size parameter of the outer sphere and a_n and b_n are the scattering coefficients given in Eqs. (7) and (8). For the infinity sums $\sum_{n=1}^{\infty}$, we use the upper limit $N_{\rm max} = \max(y + 4y^{1/3} + 2, m_1 y, m_2 y)$ [1, 37]. To avoid instabilities in the calculation of the products between spherical Bessel and Neumann functions with complex arguments, the

Aden-Kerker coefficients must be rewritten as [1]:

$$a_n = \frac{\left(\widetilde{D}_n/\widetilde{m}_2 + n/y\right)\psi_n(y) - \psi_{n-1}(y)}{\left(\widetilde{D}_n/\widetilde{m}_2 + n/y\right)\xi_n(y) - \xi_{n-1}(y)} , \tag{35}$$

$$b_n = \frac{\left(\widetilde{m}_2\widetilde{G}_n + n/y\right)\psi_n(y) - \psi_{n-1}(y)}{\left(\widetilde{m}_2\widetilde{G}_n + n/y\right)\xi_n(y) - \xi_{n-1}(y)} , \tag{36}$$

$$f_n = \frac{\imath m_2/\left[B_n\chi_n(m_2y) - \psi_n(m_2y)\right]}{\left(\widetilde{m}_2\widetilde{G}_n + n/y\right)\xi_n(y) - \xi_{n-1}(y)} , \tag{37}$$

$$g_n = \frac{\imath m_2/\left[A_n\chi_n(m_2y) - \psi_n(m_2y)\right]}{\left(\widetilde{D}_n + n\widetilde{m}_2/y\right)\xi_n(y) - \widetilde{m}_2\xi_{n-1}(y)} , \tag{38}$$

where the auxiliary functions are now

$$\widetilde{D}_n = \frac{D_n(m_2y) - A_n\chi_n'(m_2y)/\psi_n(m_2y)}{1 - A_n\chi_n(m_2y)/\psi_n(m_2y)} , \tag{39}$$

$$\widetilde{G}_n = \frac{D_n(m_2y) - B_n\chi_n'(m_2y)/\psi_n(m_2y)}{1 - B_n\chi_n(m_2y)/\psi_n(m_2y)} , \tag{40}$$

$$A_n = \frac{\psi_n(m_2x)\left[\widetilde{m}_2D_n(m_1x) - \widetilde{m}_1D_n(m_2x)\right]}{\widetilde{m}_2D_n(m_1x)\chi_n(m_2x) - \widetilde{m}_1\chi_n'(m_2x)} , \tag{41}$$

$$B_n = \frac{\psi_n(m_2x)\left[\widetilde{m}_2D_n(m_2x) - \widetilde{m}_1D_n(m_1x)\right]}{\widetilde{m}_2\chi_n'(m_2x) - \widetilde{m}_1D_n(m_1x)\chi_n(m_2x)} , \tag{42}$$

with the logarithmic derivative $D_n(\rho) = \mathrm{d}_\rho \ln \psi_n(\rho)$ [1, 7]. The nonmagnetic case is recovered when $m_q = \widetilde{m}_q$, $q = \{1, 2\}$ [1].

In the following, we consider two typical cases as Gao and Huang have been studied [18]: a coated sphere with dispersive core and dielectric shell, and vice versa. The surrounding medium (ϵ_0, μ_0) is assumed to be the vacuum and the radius $b = 1$ cm is chosen for the outer sphere. Note that, with this choice, we have $kb = \omega b(\epsilon_0\mu_0)^{1/2} \approx 1$, for $f \approx 5$ GHz. For the dielectric and non-dispersive material, we consider the lossless parameters $\epsilon_q/\epsilon_0 = 1.6$ and $\mu_q/\mu_0 = 1$ [18]. As discussed in [18], the curves of extinction efficiency become smoother when the dielectric shell or core are absorbing, leading to a decrease in the amplitude of

Q_{ext} as the absorption increases for $S < 0.5$ or $S > 0.5$, respectively. Here, we consider the lossless situation because the results when the core is dielectric and the shell is left-handed are quite similar to the one in which we have in the core vacuum or, more generally, the same lossless material as the surrounding medium. Besides, the average EM energy in a non-dispersive medium can exactly be determined only for weakly absorbing or lossless media [31].

Some curves of the average EM energy within the core [Fig. 1(a)] and within the shell [Fig. 1(b)], when the former is dispersive [$\epsilon_1 = \epsilon_1(\omega), \mu_1 = \mu_1(\omega)$] and the latter is a lossless dielectric ($\epsilon_2/\epsilon_0 = 1.6, \mu_2/\mu_0 = 1$), are presented as functions of the frequency and the thickness parameter. In Fig. 1(a), we observe in the left-handed region (4 to 6 GHz) a strong enhancement of the EM energy in the metamaterial core. This is related to the presence of standing waves inside the particle. Below and above this frequency range, the internal energy decreases monotonically. This decrease is expected for right-handed frequencies [$\text{Re}(m_1) > 0$], since there are no resonance peaks in the internal energy at the Rayleigh size parameters region ($ka < kb \leq 1$) unless the scatterer exhibits high absolute values of permeability or permittivity [26, 33], which is not the case for $f < 3.5$ GHz and $f > 6$ GHz. Besides, once in this range $\epsilon_1'(\omega) < 0$ or $\mu_1'(\omega) < 0$, but not both, we have $\text{Re}(m_1) \approx 0$ for low absorption, and the EM waves cannot propagate inside the core, but just excite resonantly surface plasmon-polaritons, like the resonance peak between 3.5 GHz and 4 GHz [17]. These surface modes contributes to the enhancement of the EM energy within the dielectric shell, as can be observed in Fig. 1(b). With increasing the thickness ratio S, the energy within the dielectric shell increases with maximum values in the left- and right-handed regions, both

associated with resonance surface modes [17].

Adding the EM energies $W_1(0,a)$ and $W_2(a,b)$ from Figs. 1(a) and 1(b) by means of Eq. (33), we have obtained the profiles of the effective EM energy within the coated sphere presented in Fig. 1(c). Note that the energy-enhancement factor $W_{\rm nor}$ is an increasing function at the left-handed region, becoming broader and with greater magnitude, as the thickness parameter S is increased, which is the opposite of Fig. 1(a). This is explicitly shown in Fig. 2 for some frequencies in the left-handed range. The same behavior can also be observed for the extinction efficiency, as we show in Fig. 3(a). These results for $b = 1$ cm are quite different from those obtained by Gao and Huang for $b = 10$ cm [18], where the amplitudes of the extinction efficiencies decrease with S.

In the extinction spectra, as discussed by Ruppin [17], the plasmon-like and the magnetic excitations reinforce each other in the low-frequency region below ω_0. In this region, the real part of the permittivity is negative, whereas the permeability has positive real part $[\epsilon_1'(\omega) < 0, \mu_1'(\omega) > 0]$. Since these two mechanisms can be considered as roughly independent, the peaks below ω_0 are provided by the contributions of the magnetic bulk polaritons and surface plasmon-polaritons, where these latter are due to resonances in the Aden-Kerker coefficient a_n. However, just above ω_0, both the electric permittivity and magnetic permeability have negative real parts, and the surface plasmon-polaritons and magnetic surface polaritons, which are due to resonances in the multipole moments a_n and b_n, respectively, suppress each other. Physically, this happens because, except for small intrinsic absorption, the metamaterial becomes transparent in this left-handed region and, thereby, no surface modes can exist [17].

The enhancement of the field intensity inside the scatterer affects the transport properties in the surrounding medium. Van Tiggelen et al. [38] have shown that, for simple three-dimensional scatterers, the energy-transport velocity $v_{\rm E}$ in the multiple scattering regime is related to the energy-enhancement factor W/W_0 by the expression $v_{\rm E} \approx c_0/[1 + f_{\rm pack}(W/W_0 - 1)]$, where c_0 is the wave velocity in the host medium (ϵ_0, μ_0) and $f_{\rm pack}$ is the volume fraction occupied by the scatterers. This expression for $v_{\rm E}$ is a good approximation for $y, \max(m_1 y, m_2 y) > 1$, that is, out of the Rayleigh size parameters region [38]. Specially, the quantity $v_{\rm E}$ is associated with the radiation diffusion coefficient $D = v_{\rm E}\ell^\star/3$, where $\ell^\star$ is the transport mean free path [38]. In Fig. 3(b), we consider a random distribution of identical metamaterial coated spheres in the medium (ϵ_0, μ_0), assumed to be the free-space, with a packing fraction $f_{\rm pack} = 0.36$, which is the same used in the experiments with nonmagnetic scatterers TiO_2 [38]. The EM energy stored inside the scatterers in the left-handed region favors small values of the energy-transport velocity, which is broader and smaller with increasing S, *i.e.*, the size parameter of the inner sphere $ka = kbS$.

Now we consider the reciprocal situation: the coated sphere is made of a lossless dielectric core $(\epsilon_1/\epsilon_0 = 1.6, \mu_1/\mu_0 = 1)$ and a wires-SRR metamaterial shell $[\epsilon_2 = \epsilon_2(\omega), \mu_2 = \mu_2(\omega)]$, given by Eqs. (29) and (30). Once again, we assume $b = 1$ cm and consider the same parameters we have used above for the dispersive metamaterial, leading a left-handed range of frequencies 4 to 6 GHz. Curves of the time-averaged EM energy within the spherical core and shell as functions of the incident frequency, for some thickness ratios, are presented in Figs. 4(a) and 4(b), respectively.

In Fig. 4(b), we note that the resonance peaks inside the metamaterial shell are shifted to low-frequencies with increasing the amount of dielectric material within the coated sphere. Specially, the EM energy within the dielectric core is strongly suppressed in the low-frequency range $\omega < \omega_0$, with minimum in $f_0 = 4$ GHz [Fig. 4(a)]. This behavior is due to the excitation of surface plasmon-polaritons in the metamaterial shell at this frequency range, which provides highest values of EM field intensity at the surface of the sphere and they decay evanescently towards its center. Thereby, for "skin depth" smaller than the layer thickness $(b - a)$, the EM field barely reaches the dielectric core, and this is clearly seen in Fig. 4. It is important to point out that this result can only be obtained by means of a direct computation of the stored EM fields in the core and shell separately, emphasizing the importance of the present analysis. The effective EM energy inside the coated sphere is shown in Figs. 4(c) and 5, where we can observe a decrease of the EM energy in the left-handed region with the thickness parameter S. The same behavior is also found in the extinction spectra, as we show in Fig. 6(a).

Using the Van Tiggelen's approach to estimate the energy-transport velocity [38], we have obtained the curves in Fig. 6(b) for a packing fraction $f_{\text{pack}} = 0.36$. Once again, the resonance peaks in the internal energy favor low energy-transport velocities in the disordered media consisting of coated particles with dielectric core and dispersive metamaterial shell. At the left-handed band, the values of energy-transport velocity are minimum for $S \leq 0.7$. With increasing the thickness parameter, above $S = 0.7$, the minimum values of v_{E}/c_0 are shifted to low-frequencies and become more separated, in such a manner that the values oscillate in the left-handed region. This behavior is easily observed in the associated extinction efficiency

for the single scattering, which is depicted in Fig. 6(a).

6. Conclusions

We have analytically calculated an exact expression for the time-averaged EM energy within a coated sphere, irradiated by a plane wave, using the explicit expressions for the EM fields inside the core and the shell separately. Although one can infer some properties of the internal energy and power loss in metamaterial coated spheres from the analysis of the extinction and scattering efficiencies, a direct computation of the stored EM fields in the core and shell separately allows a complete understanding of the behavior of EM energy density in such systems. Here, we have shown some profiles of the internal energy for two situations involving a metamaterial coated sphere: the dielectric shell and dispersive metamaterial core, and vice versa. For the metamaterial, we have used realistic dispersion relations for dispersive and lossy split-ring resonators. Finally, by means of the effective average EM energy, we have calculated the energy-transport velocity in a disordered medium consisting of metamaterial coated spheres.

Acknowledgments

The authors acknowledge the Brazilian agencies for support. TJA holds grants from Fundação de Amparo à Pesquisa do Estado de São Paulo (FAPESP) (2008/02069-0 and 2010/10052-0) and ASM from Conselho Nacional de Desenvolvimento Científico e Tecnológico (CNPq) (305738/2010-0 and 476722/2010-1).

References

1. C. F. Bohren and D. R. Huffman, *Absorption and Scattering of Light by Small Particles* (Wiley, 1983).
2. H. C. van de Hulst, *Light Scattering by Small Particles* (Dover, 1980).
3. M. I. Tribelsky and B. S. Luk'yanchuk, "Anomalous light Scattering by small particles," Phys. Rev. Lett. **97**, 263902 (2006).
4. M. Bashevoy, V. Fedotov, and N. Zheludev, "Optical whirlpool on an absorbing metallic nanoparticle," Opt. Express **13**, 8372-8379 (2005).
5. Z. Ruan and S. Fan, "Superscattering of light from subwavelength nanostructures," Phys. Rev. Lett. **105**, 013901 (2010).
6. S. A. Maier, *Plasmonics: Fundamentals and Applications* (Springer, 2007).
7. A. L. Aden and M. Kerker, "Scattering of electromagnetic waves from two concentric spheres," J. Appl. Phys. **22**, 1242-1246 (1951).
8. P.-O. Chapuis, M. Laroche, S. Volz, and J.-J. Greffet, "Radiative heat transfer between metallic nanoparticles," Appl. Phys. Lett. **92**, 201906 (2008).
9. A. E. Miroshnichenko, "Off-resonance field enhancement by spherical nanoshells," Phys. Rev. A **81**, 053818 (2010).
10. M. A. Noginov, G. Zhu, A. M. Belgrave, R. Bakker, V. M. Shalaev, E. E. Narimanov, S. Stout, E. Herz, T. Suteewong, and U. Wiesner, "Demonstration of a spaser-based nanolaser," Nature **460**, 1110-1112 (2009).
11. D.R. Smith, W. J. Padilla, D. C. Vier, S. C. Nemat-Nasser, and S. Schultz, "Composite medium with simultaneously negative permeability and permittivity," Phys. Rev. Lett.

84, 4184-4187 (2000).

12. D. R. Smith, J. B. Pendry, and M. C. K. Wiltshire, "Metamaterials and negative refractive index," Science **305**, 788-792 (2004).

13. C. Enkrich, M. Wegener, S. Linden, S. Burger, L. Zschiedrich, F. Schmidt, J. F. Zhou, Th. Koschny, and C. M. Soukoulis, "Magnetic metamaterials at telecommunication and visible frequencies," Phys. Rev. Lett. **95**, 203901 (2005).

14. W. Cai, U. K. Chettiar, H. K. Yuan, V. C. de Silva, A. V. Kildishev, V. P. Drachev, and V. M. Shalaev, "Metamagnetics with rainbow colors," Opt. Express **15**, 3333-3341 (2007).

15. J. B. Pendry, D. Shurig, and D. R. Smith, "Controlling electromagnetic fields," Science **312**, 1780-1782 (2006).

16. U. Leonhardt, "Optical conformal mapping," Science **312**, 1777-1780 (2006).

17. R. Ruppin, "Extinction properties of a sphere with negative permittivity and permeability," Solid State Comm. **116**, 411-415 (2000).

18. L. Gao and Y. Huang, "Extinction properties of a coated sphere containing a left-handed material," Opt. Comm. **239**, 25-31 (2004).

19. A. E. Miroshnichenko, "Non-Rayleigh limit of the Lorenz-Mie solution and suppression of scattering by spheres of negative refractive index," Phys. Rev. A **80**, 013808 (2009).

20. , S. A. Tretyakov, "Electromagnetic field energy density in artificial microwave materials with strong dispersion and loss," Phys. Lett. A **343** 231-237 (2005).

21. A. D. Boardman and K. Marinov, "Electromagnetic energy in a dispersive metamaterial," Phys. Rev. B **73**, 165110 (2006).

22. P. G. Luan, "Power loss and electromagnetic energy density in a dispersive metamaterial medium," Phys. Rev. E **80**, 046601 (2009).

23. P. G. Luan, Y. T. Wang, S. Zhang, and X. Zhang, "Electromagnetic energy density in a single-resonance chiral metamaterial," Opt. Lett. **36**, 675-677 (2011).

24. A. Bott and W. Zdunkowski, "Electromagnetic energy within dielectric spheres," J. Opt. Soc. Am. A **4**, 1361-1365 (1987).

25. R. Ruppin, "Electromagnetic energy in dispersive spheres," J. Opt. Soc. Am. A **15**, 524-527 (1998).

26. T. J. Arruda and A. S. Martinez, "Electromagnetic energy within a magnetic sphere," J. Opt. Soc. Am. A **27**, 992-1001 (2010).

27. R. Ruppin, "Electric and magnetic energies within dispersive metamaterial spheres," J. Opt. **13**, 095101 (2011).

28. M. Kerker, D. S. Wang, and C. L. Giles, "Electromagnetic scattering by magnetic spheres," J. Opt. Soc. Am. **73**, 765-767 (1983).

29. F. A. Pinheiro, A. S. Martinez, and L. C. Sampaio, "New effects in light scattering in disordered media and coherent backscattering cone: system of magnetic particles," Phys. Rev. Lett. **84**, 1435-1438 (2000).

30. F. A. Pinheiro, A. S. Martinez, and L. C. Sampaio, "Vanishing of energy transport velocity and diffusion constant of electromagnetic waves in disordered magnetic media," Phys. Rev. Lett. **85**, 5563-5566 (2000).

31. L. D. Landau and E. M. Lifshits, *Electrodynamics of Continuous Media* (Pergamon, 1984).

32. G. N. Watson, *A Treatise on the Theory of Bessel Functions* (Cambridge Univ. Press, 1958).

33. T. J. Arruda and A. S. Martinez, "Electromagnetic energy within a magnetic infinite cylinder and scattering properties for oblique incidence," J. Opt. Soc. Am. A **27**, 1679-1687 (2010).

34. T. Kaiser, S. Lange, and G. Schweiger, "Structural resonances in a coated sphere: investigation of the volume-averaged source function and resonance positions," Appl. Opt. **33**, 7789-7797 (1994).

35. P. Markos and C. M. Soukoulis, *Wave Propagation: From Electrons to Photonic Crystals and Left-Handed Materials* (Princeton Univ. Press, 2008).

36. R. Ruppin, "Electromagnetic energy density in a dispersive and absorptive material" Phys. Lett. A. **299**, 309-312 (2002).

37. P. W. Barber and S. C. Hill, *Light Scattering by Particles: Computational Methods* (World Scientific, 1990).

38. B. A. van Tiggelen, A. Lagendijk, M. P. van Albada, and A. Tip, "Speed of light in random media," Phys. Rev. B **45**, 12233-12243 (1992).

Figures

Fig. 1: Normalized EM energy inside a coated sphere with dispersive metamaterial core $[\epsilon_1(\omega), \mu_1(\omega)]$, given by Eqs. (29) and (30), and lossless dielectric shell ($\epsilon_2/\epsilon_0 = 1.6, \mu_2/\mu_0 = 1$) as a function of the frequency $f = \omega/2\pi$, with thickness parameters $S = 0.1,\ 0.3,\ 0.5,\ 0.9$. **(a)** EM energy $W_1(0,a)/W_0(0,a)$ inside the core $[\epsilon_1(\omega), \mu_1(\omega)]$. **(b)** EM energy $W_2(a,b)/W_0(a,b)$ inside the shell (ϵ_2, μ_2). **(c)** Effective EM energy $W_{\rm nor} = W_{1;2}/W_0$ inside the scatterer (core and shell). These quantities have been numerically calculated in the interval $2 \leq f \leq 7$ GHz, with increment $\delta(f) = 2.5 \times 10^{-2}$ GHz.

Fig. 2: Normalized EM energy $W_{\rm nor} = W_{1;2}/W_0$ inside a coated sphere with dispersive metamaterial core $[\epsilon_1(\omega), \mu_1(\omega)]$, given by Eqs. (29) and (30), and lossless dielectric shell ($\epsilon_2/\epsilon_0 = 1.6, \mu_2/\mu_0 = 1$) as a function of the thickness ratio $S = a/b$ for some frequencies in the left-handed region. These quantities have been numerically calculated in the interval $0 < S < 1$, with increment $\delta(S) = 5 \times 10^{-3}$.

Fig. 3: Coated sphere with dispersive metamaterial core $[\epsilon_1(\omega), \mu_1(\omega)]$, given by Eqs. (29) and (30), and lossless dielectric shell ($\epsilon_2/\epsilon_0 = 1.6, \mu_2/\mu_0 = 1$), with thickness parameters $S = 0.1,\ 0.3,\ 0.5,\ 0.9$. **(a)** Extinction efficiency $Q_{\rm ext}$ and **(b)** energy-transport velocity $v_{\rm E}/c_0$ through the medium (ϵ_0, μ_0) containing a packing fraction $f_{\rm pack} = 0.36$ as a function of the frequency $f = \omega/2\pi$.

Fig. 4: Normalized EM energy inside a coated sphere with lossless dielectric core ($\epsilon_1/\epsilon_0 = 1.6, \mu_1/\mu_0 = 1$) and dispersive metamaterial shell $[\epsilon_2(\omega), \mu_2(\omega)]$, given by Eqs. (29)

and (30), as a function of the frequency $f = \omega/2\pi$, with thickness parameters $S = 0.1$, 0.5, 0.7, 0.9. **(a)** EM energy $W_1(0,a)/W_0(0,a)$ inside the core (ϵ_1, μ_1). **(b)** EM energy $W_2(a,b)/W_0(a,b)$ inside the shell $[\epsilon_2(\omega), \mu_2(\omega)]$. **(c)** EM energy $W_{\rm nor} = W_{1;2}/W_0$ inside the scatterer (core and shell).

Fig. 5: Normalized EM energy $W_{\rm nor} = W_{1;2}/W_0$ inside a coated sphere with lossless dielectric core $(\epsilon_1/\epsilon_0 = 1.6, \mu_1/\mu_0 = 1)$ and dispersive metamaterial shell $[\epsilon_1(\omega), \mu_1(\omega)]$, given by Eqs. (29) and (30), as a function of the thickness ratio $S = a/b$ for some frequencies in the left-handed region.

Fig. 6: Coated sphere with lossless dielectric core $(\epsilon_1/\epsilon_0 = 1.6, \mu_1/\mu_0 = 1)$ and dispersive metamaterial shell $[\epsilon_2(\omega), \mu_2(\omega)]$, given by Eqs. (29) and (30), with thickness parameters $S = 0.1$, 0.5, 0.7, 0.9. **(a)** Extinction efficiency $Q_{\rm ext}$ and **(b)** energy-transport velocity $v_{\rm E}/c_0$ through the medium (ϵ_0, μ_0) containing a packing fraction $f_{\rm pack} = 0.36$ as a function of the frequency $f = \omega/2\pi$.

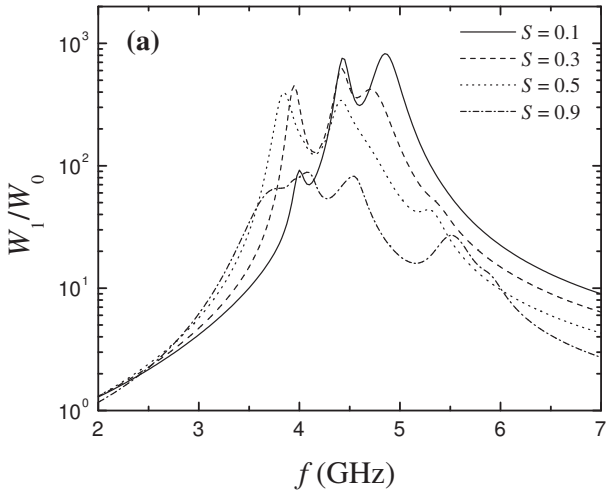
(a)
S = 0.1
S = 0.3
S = 0.5
S = 0.9
W1/W0
f (GHz)

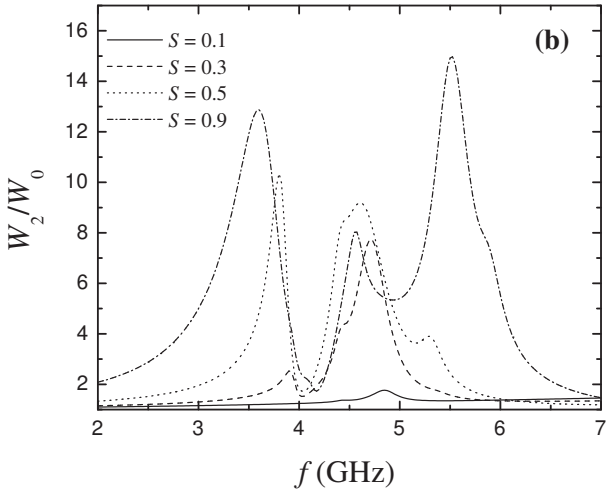
(b)
S = 0.1
S = 0.3
S = 0.5
S = 0.9
W2/W0
f (GHz)

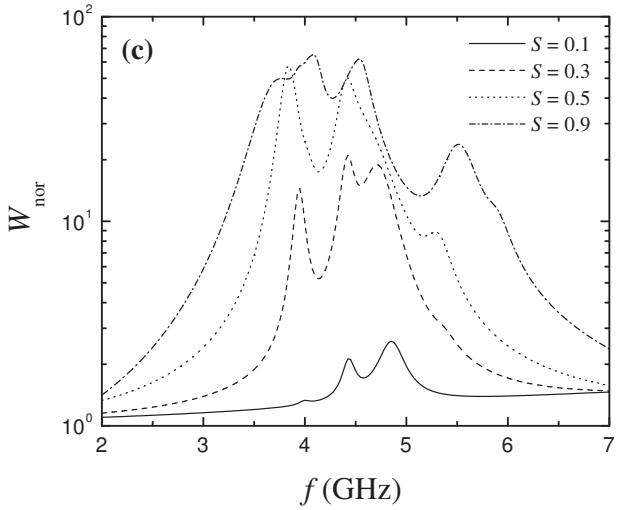
(c)
S = 0.1
S = 0.3
S = 0.5
S = 0.9
Wnor
f (GHz)

Figure 1.

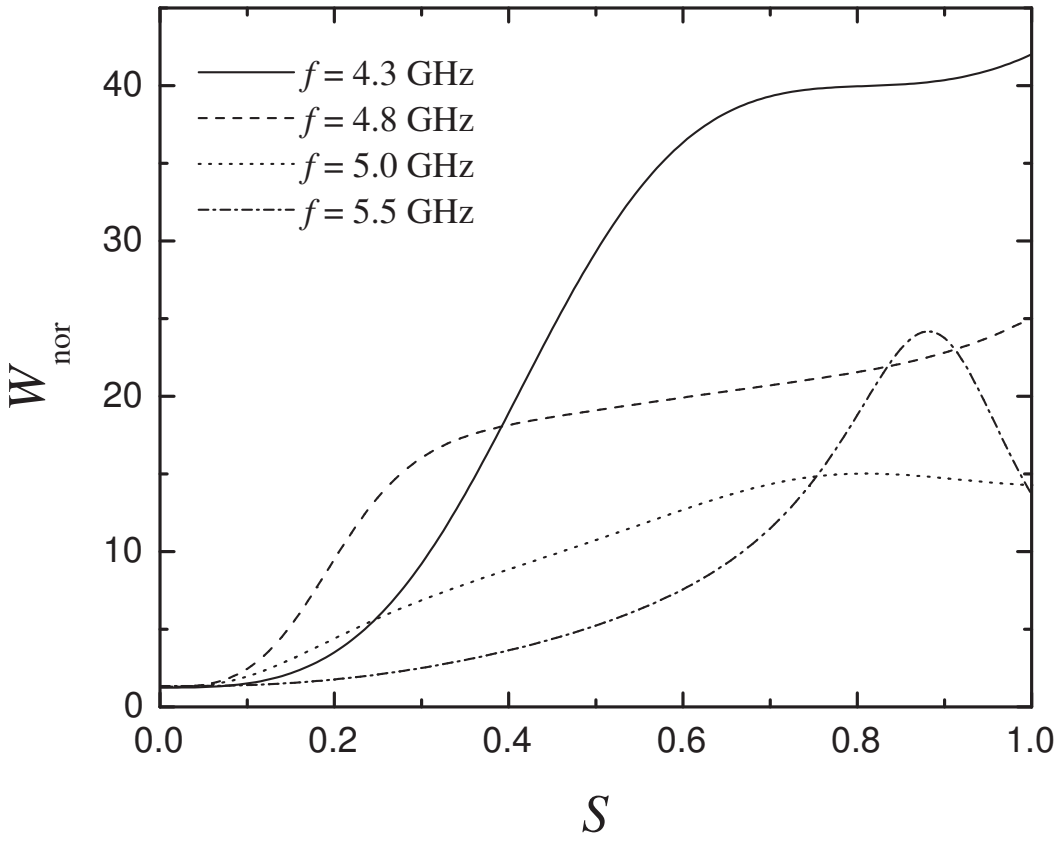
f = 4.3 GHz
f = 4.8 GHz
f = 5.0 GHz
f = 5.5 GHz
W nor
S
0
10
20
30
40
0.0
0.2
0.4
0.6
0.8
1.0

Figure 2.

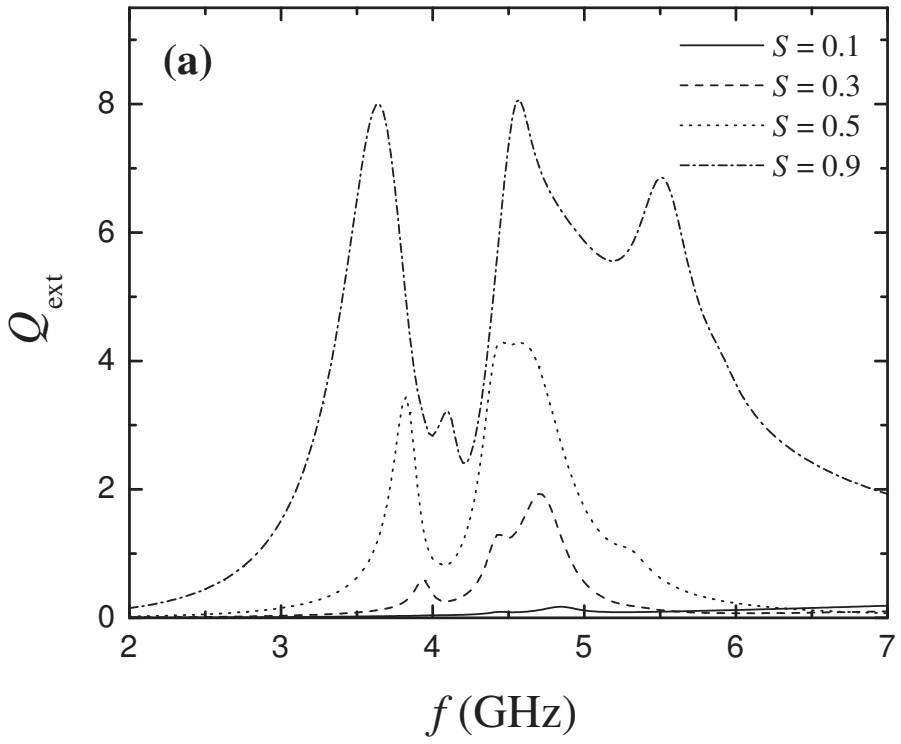
(a)
S = 0.1
S = 0.3
S = 0.5
S = 0.9
Q ext
f (GHz)

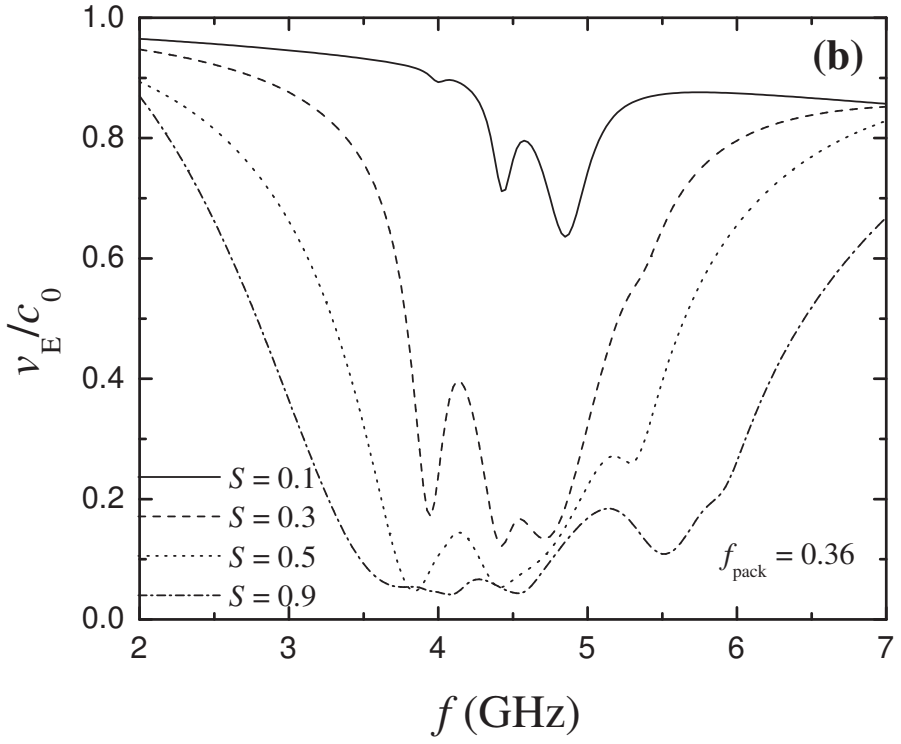
(b)
v E /c 0
S = 0.1
S = 0.3
S = 0.5
S = 0.9
f pack = 0.36
f (GHz)

Figure 3.

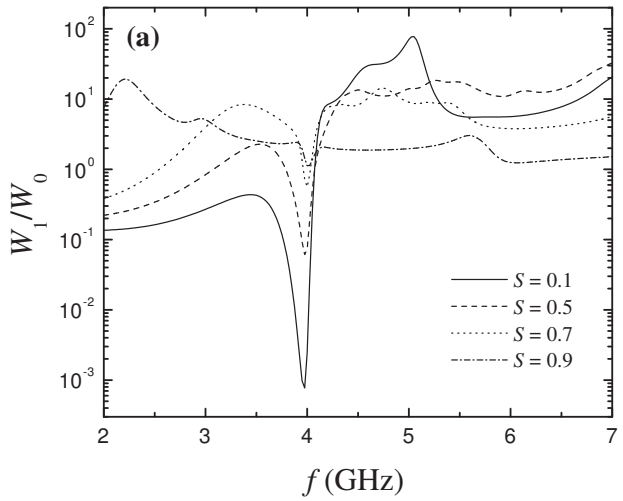
(a)
W_1/W_0
S = 0.1
S = 0.5
S = 0.7
S = 0.9
f (GHz)

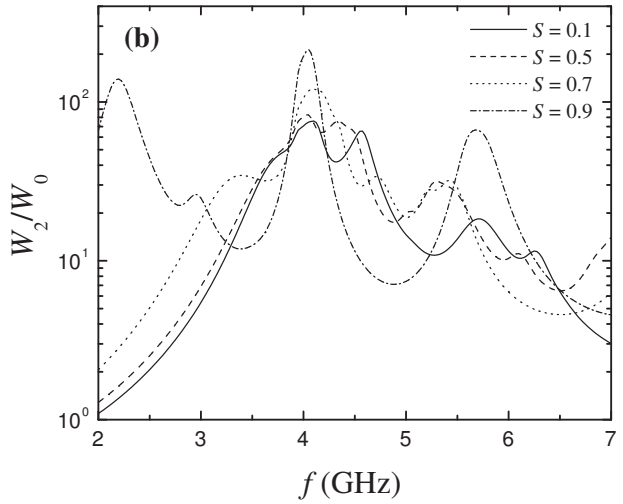
(b)
W_2/W_0
S = 0.1
S = 0.5
S = 0.7
S = 0.9
f (GHz)

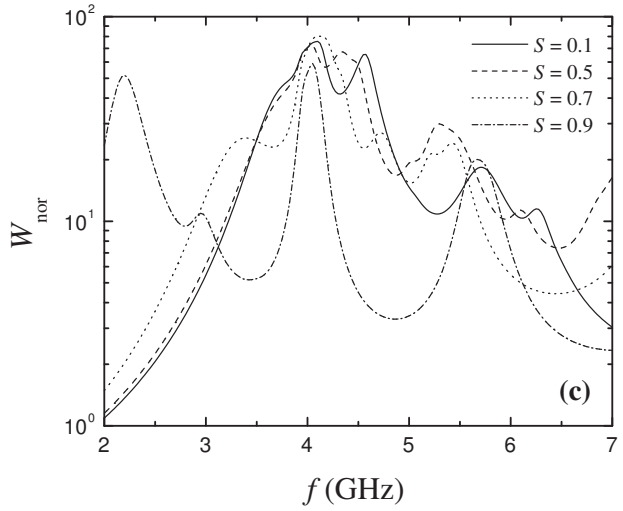
W_{nor}
S = 0.1
S = 0.5
S = 0.7
S = 0.9
(c)
f (GHz)

Figure 4.

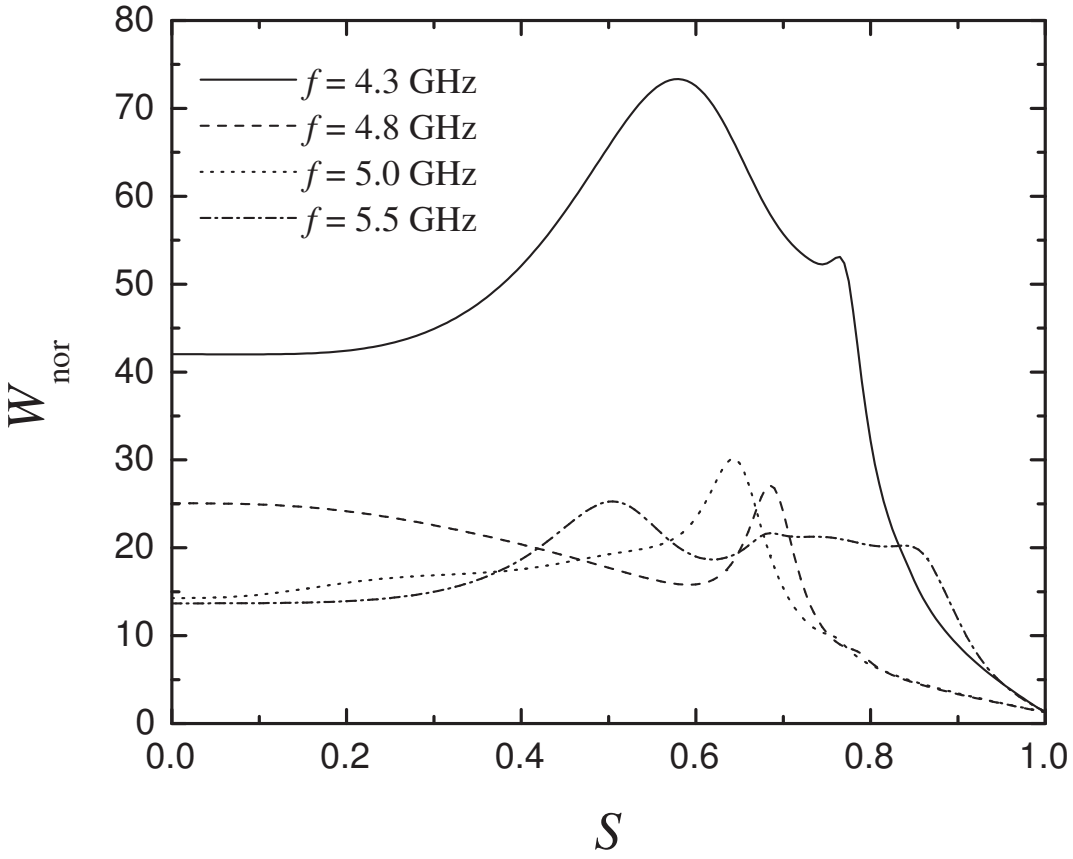
80
70
60
50
40
30
20
10
0
0.0
0.2
0.4
0.6
0.8
1.0
W_{nor}
S
f = 4.3 GHz
f = 4.8 GHz
f = 5.0 GHz
f = 5.5 GHz

Figure 5.

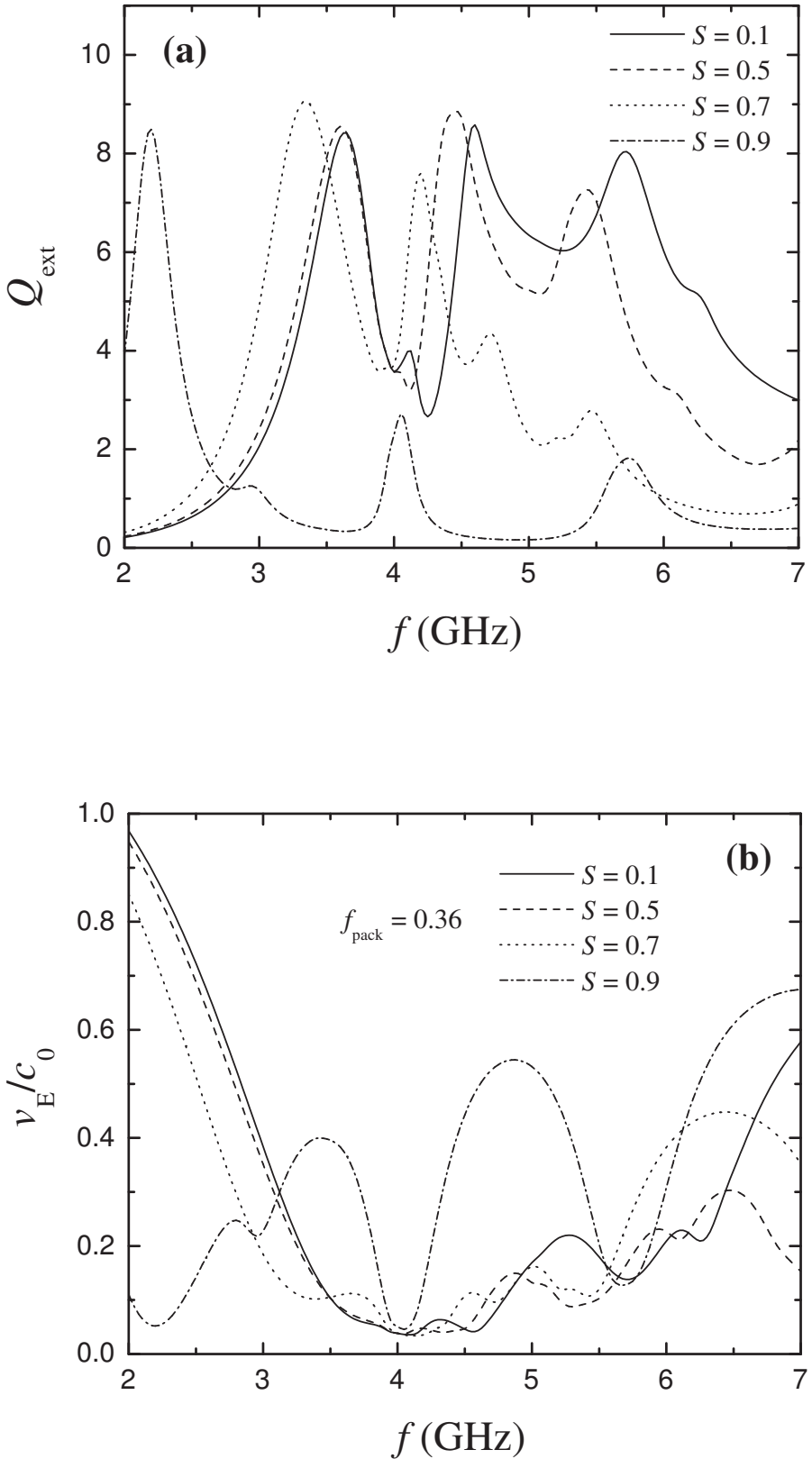

Figure 6.